

Distortion Inside a Piston Bore

Teimuraz Bardzimashvili
James F. Kelly
Elene Romelashvili

April 28, 2004

Abstract: Inside of an engine block are piston bores and corresponding piston rings. Before and during engine operation, the cylinder bore may distort, possibly causing a loss of the “light-tight” seal between the ring and the piston. We examine the conformability of elastic piston rings to a distorted cylinder bore. Several bounds exist that give the maximum bore distortion for each Fourier harmonic: the Dunaevsky, the GOETZE and the Tomanik bounds. By considering the complete bore profile, we analyze ring conformability in the presence of multiple orders of distortion with our RINGPACK program. We scrutinize the underlying assumptions for each bound. We then test our RINGPACK simulator with Finite Element (FE) data and compare our results to each bound. Our results indicate that the GOETZE bounds predict conformability more accurately than the Dunaevsky bounds at high orders of distortion.

Table of Contents

Introduction.....	3
Definitions and Bound Assumptions.....	4
Comparison of Bounds.....	7
Finite Element (FE) Data and Ring Specifications.....	10
RINGPACK Description	13
Boundary Conditions.....	14
Curvature of Free Ring.....	15
Curvature of Cylinder Bore.....	16
Pressure Calculation.....	16
Results.....	17
Parameter Study.....	17
Analysis of FE Data.....	18
Discussion.....	20
Recommendations.....	22
Future Work.....	22
Acknowledgements.....	22
References.....	23
Appendix A: Free Shape Problem.....	25
Appendix B: GOETZE Bound Deviation	28
Appendix C: Three-Dimensional Distortion.....	30
Appendix D: RINGPACK Code.....	32

Introduction

Inside of an engine block are piston bores and corresponding piston rings. The piston ring may be viewed as a C-shaped, structural elastic beam that makes contact with the walls of the piston bore. The piston ring is guided into a groove around the piston as the piston-ring assembly is inserted into a cylinder of the engine block. The C-shaped ring is forced closed, so that the C-shape becomes roughly a circle surrounding the piston. Because the ring wants to revert to its “free” shape, it exerts a pressure on the cylinder walls. Ideally, the piston ring forms a “light-tight” seal with the surrounding cylinder wall and piston, meaning that no gaps are present through which combustion gasses can escape.

In a typical assembly, there are three rings: two compression rings and an oil control ring. The compression rings seal a piston in its combustion chamber, so that pressure from exploding gasoline can be converted to mechanical energy. Also, the rings assist the dissipation of heat through the cylinder wall and regulate oil consumption. For a detailed discussion of piston ring functionality, see [1] and [2].

Due to imperfections in design and assembly, gas pressure and thermal variations, the cylinder may distort before and during operation. Hence, the circular piston ring must conform to a slightly imperfect cylinder bore. Since the piston ring acts like an elastic beam [3], we expect the ring to successfully conform to a slightly distorted bore. However, if these distortions become too large, the ring may be unable to conform and lose its “light-tight” seal with the cylinder wall and piston. This seal breach may result in increased oil consumption and leakage, blowby, and engine wear; also fuel efficiency may decrease [4, 5]. Hence, we consider the *conformability* problem in this report: Given distortions in the cylinder bore and a set of piston ring specifications, determine if the ring forms a “light-tight” seal.

Many researchers have attacked the conformability problem using both analytical and computational tools. Early analytical work includes pioneering work by Prescott, Timoshenko, and Englisch [6,7,8]. Gintsburg [9] analyzed *splitless rings* (rings with no gap) by approximating distortions from the nominal radius r_0 with a Fourier series. Letting $\xi(\phi)$ denote the measured bore shape (where ϕ is the polar angle), $\xi(\phi)$ is approximated by

$$\xi(\phi) \approx r_0 + \sum_{k=1}^N A_k \cos(k(\phi + \delta_k)), \quad (1)$$

where k is the *order* and δ_k is a *phase angle*. By assuming a bore profile in this form, Gintsburg derived a set of bounds for each Fourier harmonic of distortion. More recently, Müller [10] and Dunaevsky [11] have derived competing bounds on each harmonic. GOETZE AG adopted the Müller bounds in their *Incometer* cylinder distortion measurement system [12].

Realizing the limitations of the analytical methods, automotive researchers have begun developing Finite Element (FE) models of piston ring dynamics. These models [13, 14, 15] take into account gas pressure, oil lubrication and complicated three-dimensional distortions that the above analytical models neglect. Recently, Dunaevsky [16,17,18,19,20] has begun work on a three-dimensional model of the piston ring that does not assume a constant cross-section. This model takes into account torsion and twist of the ring. However, the theory behind this three-dimensional analysis is still poorly understood and currently under development. For background on this theory, we refer the reader to the classic work by Love [21].

Most automakers and piston ring manufacturers use either the GOETZE (or Müller) bounds or the Dunaevsky bounds. However, these bounds give different upper limits to each term in the Fourier series expansion. Moreover, these bounds, cannot predict conformability in the presence of multiple orders of distortion. This discrepancy prompted Tomanik [22] to empirically compare the bounds to inometer measurements. In this report, we follow-up on Tomanik's work and analyze the physical and mathematical assumptions underlying each set of bounds. We develop a simple program to analyze a bore profile, comparing the bounds to FE data.

Definitions and Bound Assumptions

Consider a curved, prismatic member (or *piston ring*) with height h and thickness t . For the present analysis, assume a constant, and rectangular cross-section $A = ht$. (We consider a variable cross-section later.) Assuming the ring is nearly circular, we impose a polar coordinate system (ϕ, r) about the center of the ring. We assume the ring has homogenous density and is composed of some flexible material with modulus of elasticity E . The ring is *split*, meaning that there is a gap in the free state. When the ring is compressed, this gap is reduced to a small space to allow sealing. See Figure 1. In contrast, some authors have studied the dynamics of *splitless* [9].

By applying a radial pressure $p(\phi)$ and/or bending moment $M(\phi)$ to the ring, we deform (elastically) the shape of the ring. Since the cross-section is constant, we can define an axis from each of the endpoints of the ring. By deforming the ring, we deform any of these axes. Moreover, there is a neutral axis in the ring, which remains stress free. We will measure the ring relative to this neutral axis.

The piston ring assumes a free, uncompressed state given by $\psi(\phi) = r(\phi) + u(\phi)$. By applying a radial pressure $p(\phi)$, we compress the ring to shape $r(\phi)$. Also, define the *radius of curvature* of the uncompressed ring as ρ and the curvature of the uncompressed ring as $\kappa_0 = 1/\rho$; likewise, for the compressed ring, define radius of curvature r and curvature $\kappa_1 = 1/r$.

In order to linearize the equations of elasticity, Müller and Dunaevsky make two fundamental assumptions, discussed below.

Hooke's Law: Stress is proportional to strain. Mathematically, $\sigma = E\varepsilon$, where E is the modulus of elasticity.

Thin Rod Approximation: The thickness of the ring t is much smaller than the radius of curvature ρ .

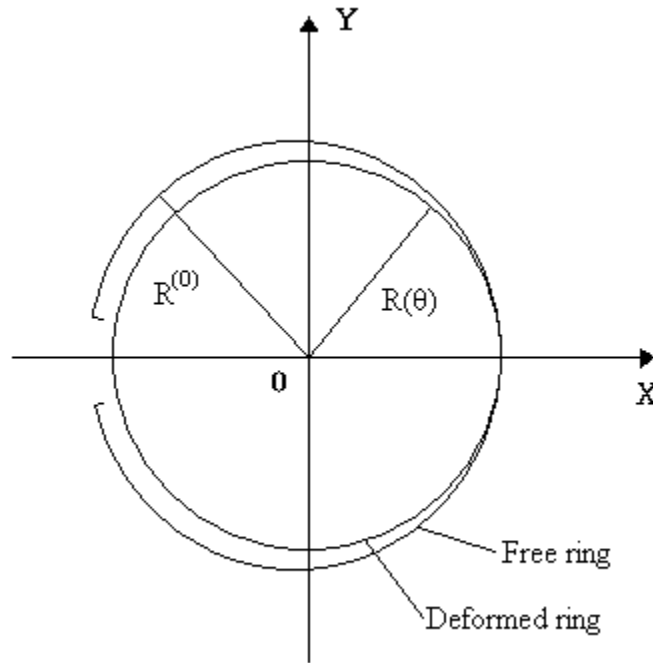


Figure 1. This schematic shows the projection of ring on the plane perpendicular to the bore axis [19].

Since bore distortions are well within the elastic limit, we are justified in applying Hooke's law. Common ring specifications [1] give $t/\rho \approx .10$, justifying the thin-rod approximation. To simplify the analysis, both Müller and Dunaevsky make a third fundamental assumption.

Radial Assumption: The bore (and hence the ring) distorts only in the radial direction. We neglect both tangential and axial distortions.

For rings with non-uniform cross-sections, this assumption does not hold. Moreover, the radial assumption may not be wholly accurate for uniform cross-section rings. Several researchers [14,19] are currently considering the effect of these complicated 3D distortions on conformability.

By combining these three assumptions, we arrive at the fundamental elastic relation:

$$\kappa_1 - \kappa_0 = \frac{M(\phi)}{EI} . \quad (2)$$

Equation 2 relates the bending of the ring to the flexural rigidity (or “stiffness”) EI to the curvature of the ring. In other words, the bending of the ring is directly proportional to the change in curvature.

In the following discussion, we wish to specify ring conformability by a single parameter. We define the *conformability coefficient* via

$$K = \frac{F_t r_m^2}{EI} , \quad (3a)$$

where F_t is the tangential force (applied at the gap) required to close the ring. Alternatively, we can define K via

$$K = \frac{p_0 h r_m^3}{EI} , \quad (3b)$$

where r_m is the middle radius (approximated by the nominal radius r_0). For most rings, K takes values between .01 and .04.

In order to derive the pressure distribution that the compressed ring exerts upon the cylinder bore, Dunaevsky makes several assumptions regarding the uncompressed ring $\psi(\phi)$.

Free Shape Approximation: The deviations $u(\phi)$ and $u'(\phi)$ are small compared to radius of curvature r . Moreover, the free shape is approximated by

$$u_f(\phi) = Kr_m(1 + .5\phi \sin \phi) . \quad (4)$$

Equation 4 and variants are widely used. However, researchers at the Engine Research Lab have developed an exact solution that does not make the Free Shape Approximation [2]. To verify this work, we solved for the free shape numerically in Appendix A. Moreover, we will demonstrate how to relax this approximation and obtain a closed-form expression for curvature.

Uniform Pressure Assumption: The ring, when inserted into a circular bore, exerts a uniform pressure.

In a private conversation with Dunaevsky, he remarked that this assumption is generally *not* true. In fact, some piston ring manufacturers (such as Riken), design rings that produce “apple” or “pear” shaped pressure distributions. In practice, the pressure distribution is very difficult to measure with any accuracy.

Superposition Assumption: The pressure distribution induced when a ring whose free shape is $r + y$ and is compressed to a perfect circle r is approximately the same as the pressure distribution induced when a ring whose free shape is $r + u$ is compressed to oval shape $r + \frac{e}{4} \cos 2(\phi + \beta)$. Moreover, each order distortion does not influence any of the other orders.

Constant Cross-Section Assumption: The cross section area A is not changed by elastic deformation. That is, the thickness and height do not change even though the neutral axis changes position.

Comparison of Bounds

In this section, we quantitatively compare the GOETZE [10], Dunaevsky [11] and Tomanik [22] bounds. Since we are interested in relating the maximum radial cylinder distortion to the pressure exerted by the ring on the bore, we wish to analyze bounds for the coefficients A_k in Equation 1. By determining the tightest set of bounds on each term, the piston ring's design characteristics can be optimized for fuel efficiency and engine durability [6].

We can represent bore distortion mathematically by a bore profile. Figure 2 shows a typical bore profile (adapted from [11]). We can decompose this profile into Fourier harmonics, thus representing the radial distortion as a Fourier series (see Equation 1). Before we discuss the bounds themselves, we interpret the various Fourier harmonics physically.

At present, many researchers consider terms beyond fourth-order to be negligible [9]; however, other experts recommend considering fifth and sixth order terms [16,17,18,19,20]. Second-order distortions in Equation 1 reflect the ovality of the distorted cylinder bore. In [9], Scheider found that these distortions depend heavily on the vertical position of the piston ring relative to the cylinder. Third-order distortions form a cloverleaf shape; machining imperfections are responsible for these distortions. Finally, excessive tightening of the tension bands in the cylinder cause fourth-order distortions. Although these distortions can be minimized, they cannot be eliminated entirely. Hence, we require an accurate theoretical bound on the distortions.

Figure 3 (reprinted from [11]) shows second, third and fourth order distortions using polar coordinates.

Using the assumptions outlined in the previous section, Dunaevsky derives a set of bounds for each Fourier harmonic. Denoting A_k as the k -th coefficient, Dunaevsky shows

$$A_k < 1.52 \frac{Q}{h} \frac{r^3}{t^3} \frac{1}{E} \frac{1}{k^2 - 1}. \quad (5)$$

In the above equation, Q is the diametrical force required to close the ring. This diametrical force is related to the force F_t required to close the ring by the theoretical formula

$$Q = 2.63F_t.$$

However, the piston manufacturer Dana Perfect Circle uses a rival empirical formula given by $Q = 2.15F_t$.

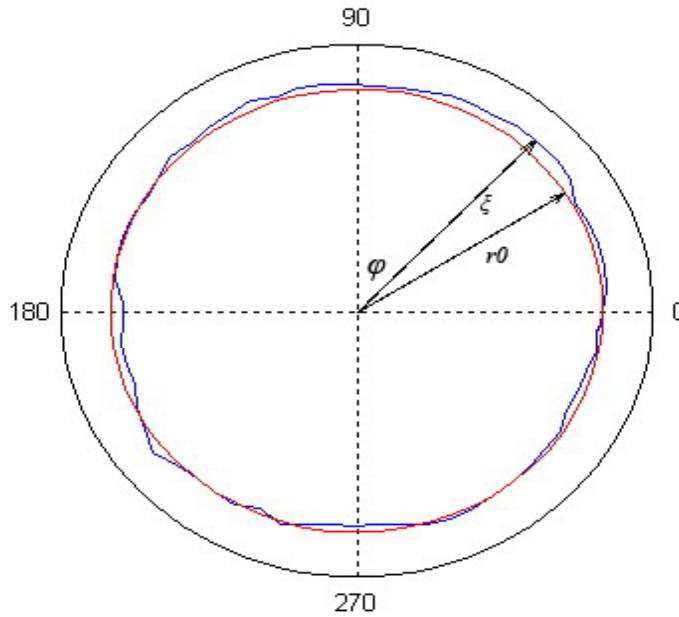


Figure 2. This graph shows bore distortion in polar coordinates.

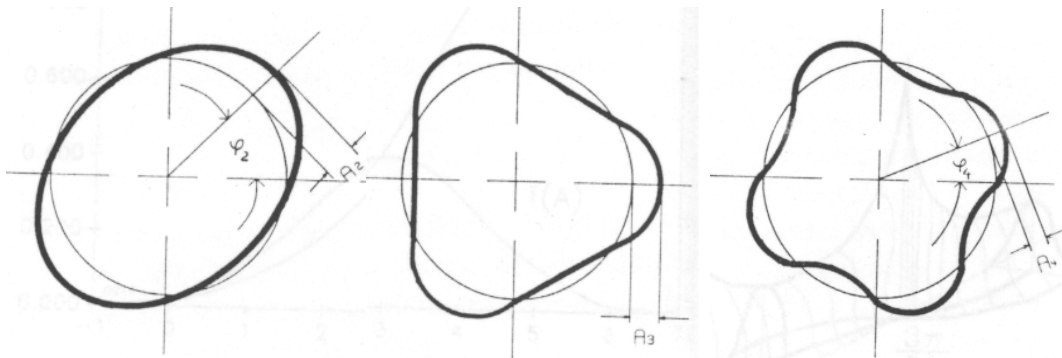


Figure 3. In these polar graphs, we display sample second, third and fourth order distortions. The original figures were printed in [11].

Prior to Dunaevsky's work, Müller derived a similar bound on each of the Fourier terms [8]. Using the notation above, we have the bound

$$A_k < 4.56 \frac{Q}{h} \frac{r^3}{t^3} \frac{1}{E} \frac{1}{(k^2 - 1)^2} . \quad (6)$$

For second-order distortions ($k=2$), Equations 5 and 6 yield the same bound. However, they deviate for higher order distortions. These deviations prompted Tomanik to derive a semi-empirical formula in [22]. Using experimental measurements and linear regression, Tomanik determined a semi-empirical formula given by

$$A_k < \frac{Kr}{20(k^2 - 1)} . \quad (7)$$

Here, K is the conformability coefficient defined by Equations 3. We summarize all three bounds in terms of K in Table 1.

Figure 4 shows the bounds for distortions up to sixth order using ring parameters supplied by DaimlerChrysler (see Table 2). Note that the GOETZE bounds are more conservative for orders three and four. Also note that both the Dunaevsky and GOETZE bounds overestimate ring conformability by a factor of six for second order deformations. Both the Tomanik and Dunaevsky bounds share the $1/(k^2-1)$ dependence. In general, all three sets of bounds show that conformability is highly sensitive to very small, high-order distortions.

The differences between Equations 5, 6 and 7 prompt several questions. Firstly, which assumptions made by Dunaevsky and GOETZE cause the overestimation of the bounds? Secondly, can we derive a tighter set of bounds by relaxing these assumptions? Finally, how should we use these bounds if we measure multiple-orders of distortion in a given bore?

Table 1. We compare the GOETZE, Dunaevsky, and Tomanik bounds via the conformability coefficient K .

GOETZE	Dunaevsky	Tomanik
$\frac{Kr_m}{(k^2 - 1)^2}$	$\frac{Kr_m}{3(k^2 - 1)}$	$\frac{Kr_m}{20(k^2 - 1)}$

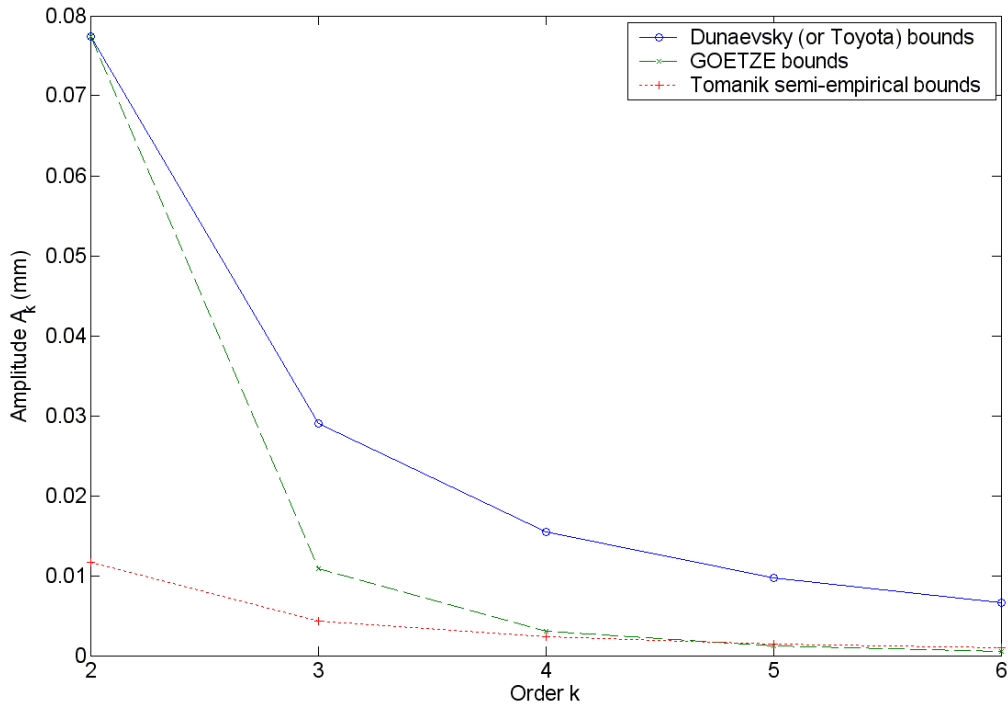


Figure 4. We compare the Dunaevsky bounds (solid), GOETZE bounds (dotted) and Tomanik (dashed) bounds.

Finite Element Data and Ring Specifications

Another approach to the ring conformability problem is Finite Element Analysis (FEA). FEA can take into account ring cross sectional properties, ring tension, pressure load above and below the ring, friction and oil flow. Researchers at the Engine Research Lab (ERL) at MSU are taking this approach [2,14,15] in development of their Cylinder Kit Analysis System for Engines (CASE). Some other engine simulation FEA code developers include AVL, Ricardo, and MIT. Although these models account for complicated ring dynamics, they are computationally expensive.

To evaluate each of the bounds and our own method, DaimlerChrysler provided their own FE data and ring specifications. The FE data specifies a computational grid and a displacement vector associated with each grid point. The grid itself is arranged in sixteen decks, each deck having approximately 23 points. To visualize this data, we map the magnitude of each displacement vector onto the grid. Figure 5 shows the various magnitude displacements, with a maximum distortion of .07 mm. Noting that the radius of the bore is 51.181 mm, this maximum displacement represents less than 0.15% of the bore radius. Also note that the cylinder is inclined at approximately 45°, much like an actual cylinder in a V-6 engine.

Table 2 displays the ring specifications provided by DaimlerChrysler. In our calculations, we used the empirical formula

$$Q = 2.15F, . \tag{8}$$

We note that this ring has a rather low conformability coefficient K .

We extracted bore profiles by calculating the radial displacement and ignoring the tangential and axial displacement. For details, see the section describing RINGPACK. Figure 6 shows raw bore profiles for decks 3, 6 and 9. We used the default linear interpolation in MATLAB to connect the marked data points. Note that the general shape of each profile is similar. Moreover, the amplitude of distortion appears to increase as we move up the cylinder bore.

Table 2. This table displays ring specifications provided by DaimlerChrysler.

Diametrical Load (N)	13.2558
Height (mm)	1.48
Thickness (mm)	3.985
Middle Radius (mm)	51.181
Young's Modulus (N/mm ²)	152 000
Closing Force (N)	6.1655
Moment of Inertia (mm ⁴)	7.8049
Stiffness (mm ²)	1 186 300
Conformability	0.0136

3D bore distortion (exaggerated)

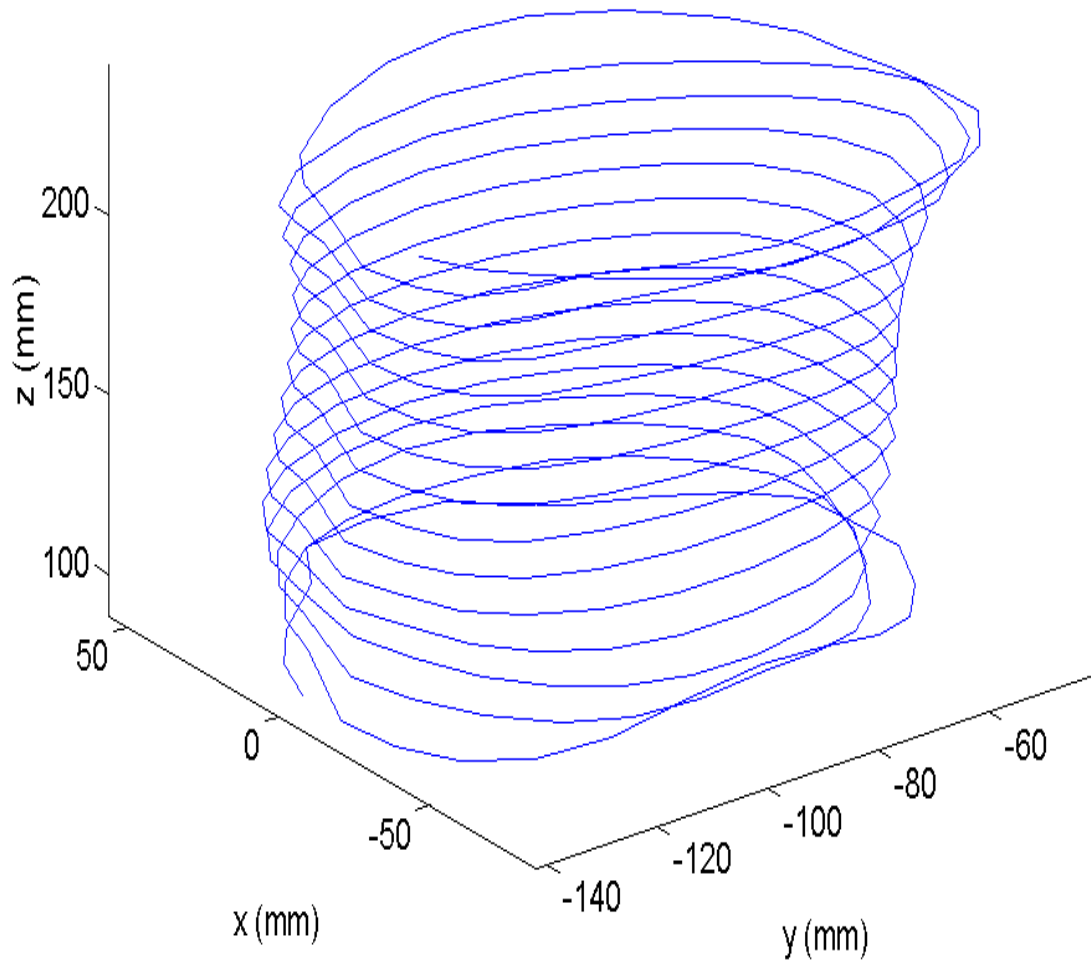


Figure 5. This figure shows the distorted bore at each grid point. Note that the bottom deck suffers from very little distortion, whereas the top deck has much larger distortion.

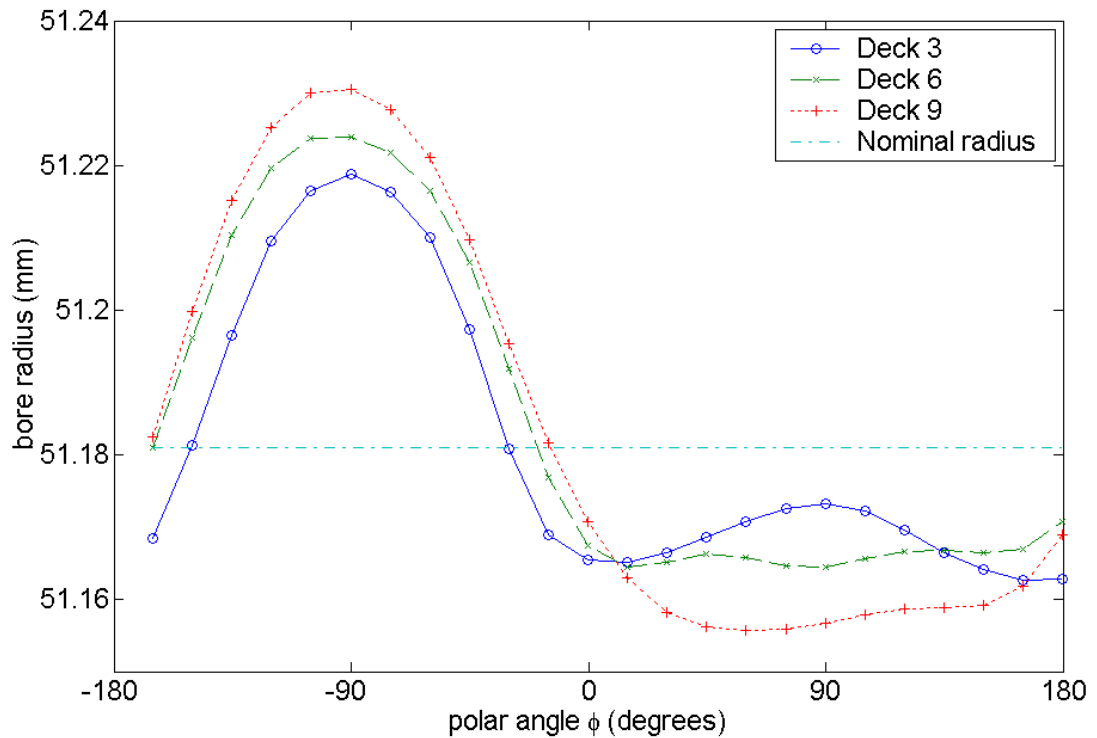


Figure 6. In this figure, we display FE Bore profiles for decks 3, 6 and 9.

RINGPACK Description

In order to test the FE data and evaluate the effectiveness of each bound, we wrote a MATLAB program called RINGPACK. See Appendix D for code. Figure 7 shows the general structure of the program.

The program has two general components: a ring component and a bore component. The ring component calculates the free shape of the ring (see Appendix A) and the curvature given specifications. The bore component imports FE data, extracts a profile, interpolates the profile, and calculates curvature. We address the curvature problem in the following sections.

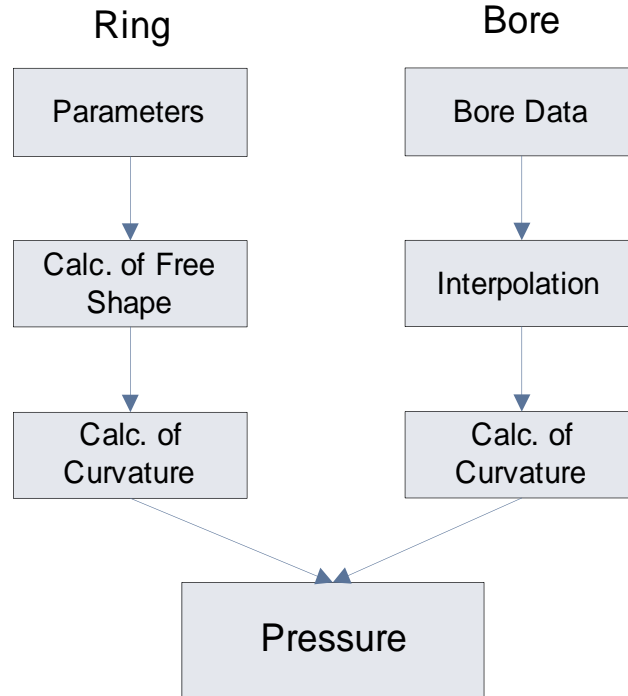


Figure 7. This figure displays the RINGPACK structure diagram.

Boundary Conditions

To determine the free curvature, we must first determine the correct boundary conditions to impose at the ends of the ring. We consider a split ring, with a small gap at the back of the ring (where $\phi = \pi, -\pi$). At the ends of the ring, the bending moment $M(\phi)$ must vanish since there is not external torque applied to the ring. In the case of constant pressure (or no radial deviations), we argue that shear force $T(\phi)$ must also vanish.

Recall that the only external force on the ring is a radial pressure acting inwards. By analyzing the forces on the ring, we can show that

$$p h r = \frac{dT}{d\phi} + N,$$

where N is the tangential force on the ring. Due to the free-end condition, the tangential force vanishes at the back of the ring. In the free case, the constant load condition implies zero shear force at the endpoints. However, in the distorted case, we would expect a non-zero shear at the endpoints.

Curvature of Free Ring

Previous work [10,11] used an approximation for the free shape of the ring (see Equation 4). However, we can increase the accuracy of our calculations by deriving the exact curvature of the free, uncompressed ring.

Consider the free ring shown in Figure 8. At each polar angle ϕ , the cylinder exerts a radial pressure $p(\phi)$. We wish to determine the bending moment $M(\phi)$ induced by this radial pressure. Fix an angle ϕ and a position vector \vec{r} and consider the small bending moment dM induced by pressure at angle ϕ' . By definition of moment,

$$d\vec{M} = \vec{r} \times d\vec{F}, \quad (9)$$

where $d\vec{F}$ is the small force associated with pressure at angle ϕ' . Since the problem is two-dimension, $d\vec{M}$ will only have a z -component. Therefore, define dM to be the z -component of $d\vec{M}$. We can then calculate

$$d\vec{F} = \vec{r}' hp(\phi') d\phi'. \quad (10)$$

Inserting Equation 10 into Equation 9 and evaluating the cross-product yields the expression:

$$dM = hr(\phi) \sin(\phi - \phi') p(\phi') r(\phi') d\phi'. \quad (11)$$

For the free-ring problem, the pressure p_0 exerted on a perfectly round bore is constant. Hence, we can integrate Equation 11 over the angle ϕ' subject to the boundary condition $M(-\pi) = 0$.

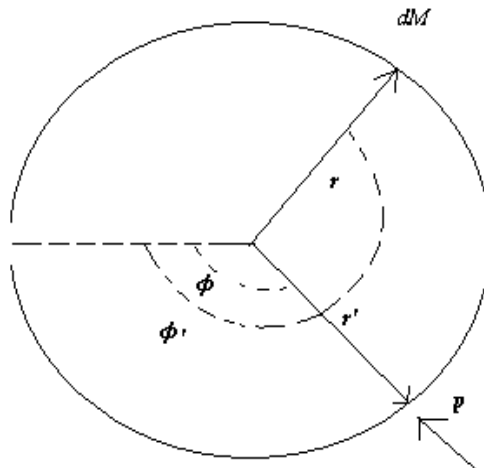


Figure 8. We use this schematic used in derivation of free shape curvature.

This integration yields the closed-form expression

$$M(\phi) = p_0 h r_m^2 (1 + \cos\phi), \quad (12)$$

where r_m is the middle radius of the cylinder. We can then determine the free curvature κ_0 by using Equation 2. Noting that final curvature $\kappa_1 = 1/r_m$, we find

$$\kappa_0 = \frac{1 - K(1 + \cos\phi)}{r_m}. \quad (13)$$

Equation 13 allows use to calculate free curvature without considering the actual free shape (approximate or exact). For readers interested in the exact free shape, please consult Appendix A or reference [2].

Curvature of Cylinder Bore

To determine the curvature of the cylinder bore, we first interpolate the bore profile with a Fourier series. Since we only have 23 data points per profile, the fast Fourier transform (FFT) does not provide enough accuracy. Moreover, the data points are irregularly spaced with respect to angle. Many methods exist to evaluate Fourier coefficients for irregularly spaced datasets [23]. We chose to interpolate the data points via a cubic spline. We then evaluate the Fourier coefficients via Gauss quadrature [24], with a variable number of Gauss abscissas. For implementation details, see the function `fcoeffs_trighi` in Appendix D. Once we calculate the Fourier coefficients, we can compute the derivatives of the Fourier series analytically. We then apply the exact, polar coordinate curvature formula

$$\kappa_1 = \frac{\xi^2 - 2\xi'^2 + \xi\xi''}{(\xi^2 + \xi'^2)^{3/2}}. \quad (14)$$

Pressure Calculation

Once the change in curvature is known, we can calculate the bending moment via Equation 2. Finally, we calculate pressure numerically using the relation:

$$p(\phi) = \frac{1}{hr^2(\phi)} \left(M + \frac{d^2M}{d^2\phi} \right). \quad (15)$$

A derivation of Equation 15 can be found in [3]. If the pressure of the ring is positive for all angles, then we assume the ring maintains a “light-tight” seal. If, however, the pressure is negative for any angle, the ring breaks the seal and conformability is lost.

Results

In order to compare our RINGPACK program with established results, we calculated bounds numerically. For each Fourier harmonic ($k = 2$ to 6), we calculated the minimum radial distortion for which pressure became negative. Figure 9 compares these RINGPACK bounds to the Dunaevsky and GOETZE bounds for the parameters in Table 2. Note that the RINGPACK bounds are virtually identical to the GOETZE bounds. This initial result suggests a hidden flaw in the Dunaevsky bounds.

Parameter Study

To aid in the design of future piston rings, we studied how varying the ring parameters effected conformability. In this analysis, we perturbed the middle radius and thickness given in Table 2 by 20% in both directions using a 31 by 31 spatial grid. We then calculated the bounds for these perturbed radii and thicknesses using second-order, radial distortions. Thus, we made the implicit assumption:

$$A_k = f(r_m, t),$$

where A_k is the bound on k -th order distortions.

Figure 10 displays bounds as a function of both thickness and radius. Note that the bounds are highly sensitive to these two variables. Realistically, a very small error in either radius or thickness could lead to a large difference in the allowable distortion.

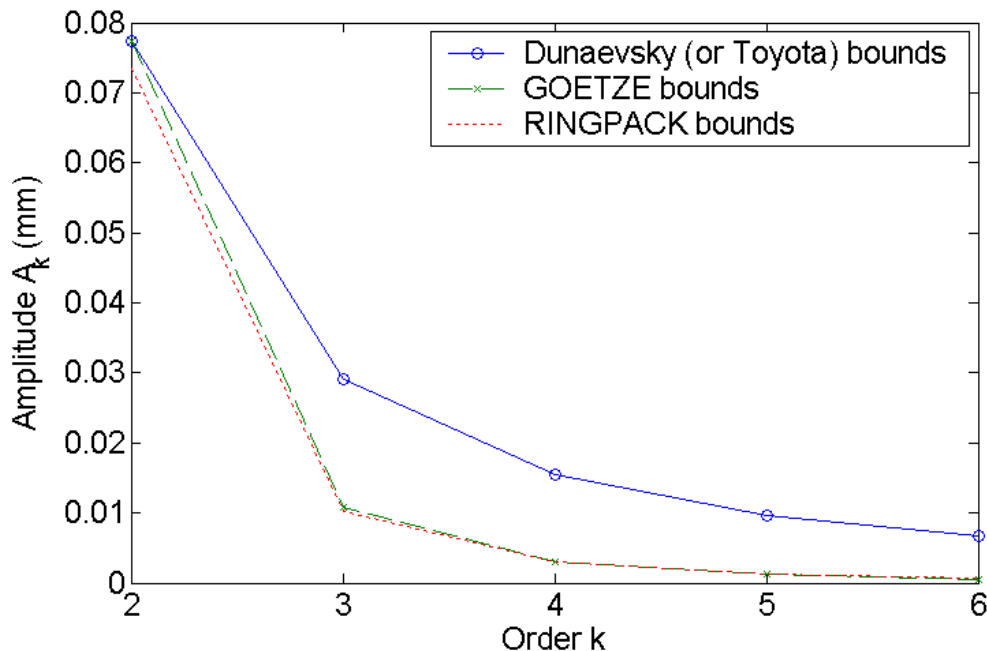


Figure 9. We compare RINGPACK bounds to Dunaevsky and GOETZE bounds.

Analysis of FE Data

We next tested the RINGPACK program with FE data. For the demonstration we chose deck 9 with 23 data points. Figure 11 shows the interpolated profile bore (with data points shown as circle) against polar angle. To interpolate, we used five terms in the Fourier series expansion. Figure 12 displays pressure distribution of the distorted ring as a function of angle. Since we are primarily interested in the sign of pressure, we also show the zero-pressure line. We see that pressure becomes negative, which indicates that the “light-tight” seal between cylinder wall and the ring is broken.

Since the standard conformability criterion is the GOETZE bounds, we also calculated the GOETZE bounds from Equation 5 using the ring parameters listed in Table 2. We plotted the computed Fourier coefficients against the GOETZE bounds in Figure 13 for orders two through five. Note that none of the Fourier coefficients exceed the GOETZE bounds. For orders beyond five, the coefficients were negligible.

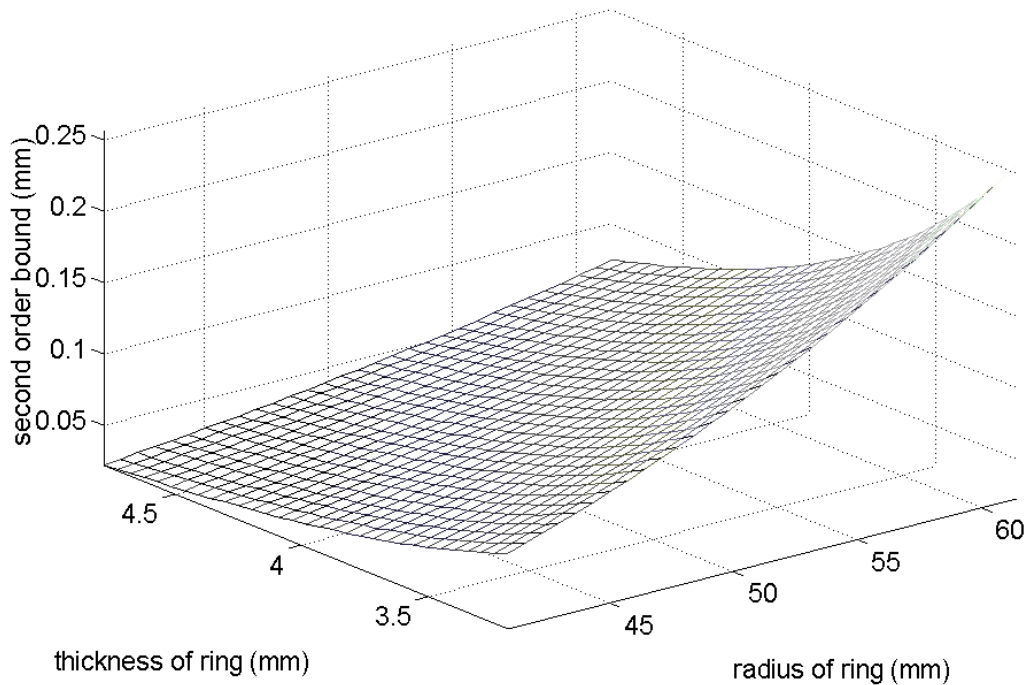


Figure 10. This figure displays second order bounds for perturbed parameters r_m and t .

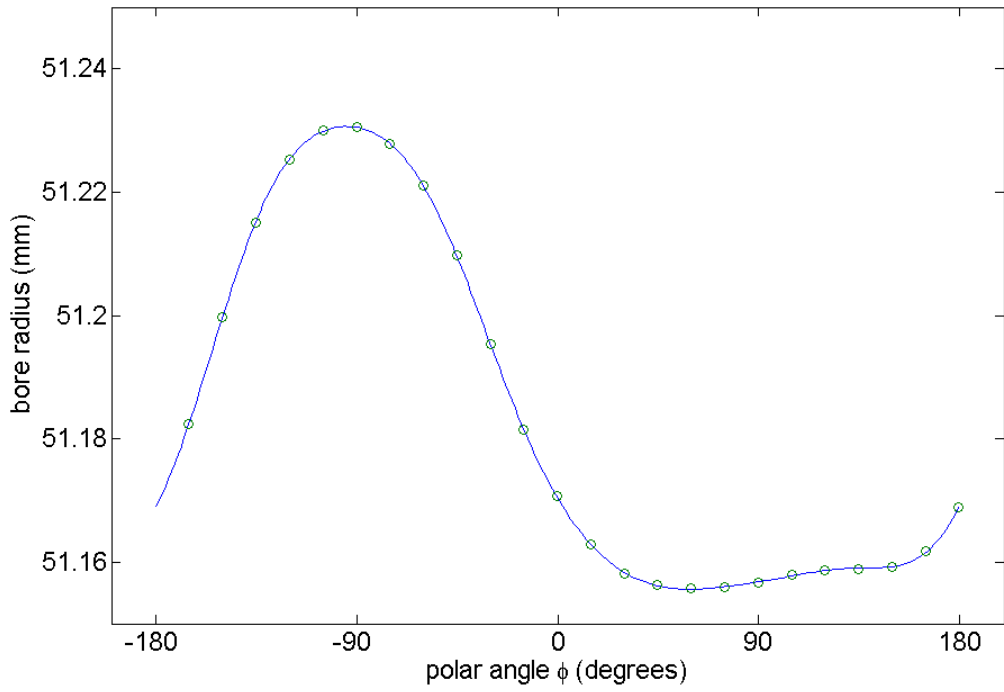


Figure 11. This figure displays the interpolated bore profile for deck 9.

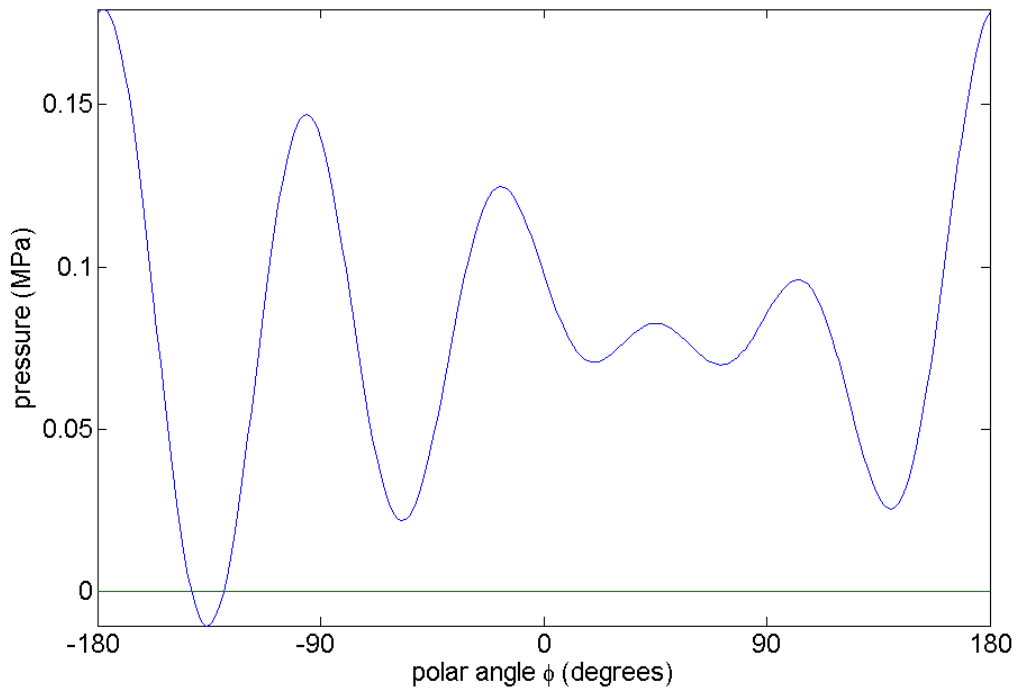


Figure 12. We display the pressure distribution of distorted ring, using the bore profile shown in Figure 11.

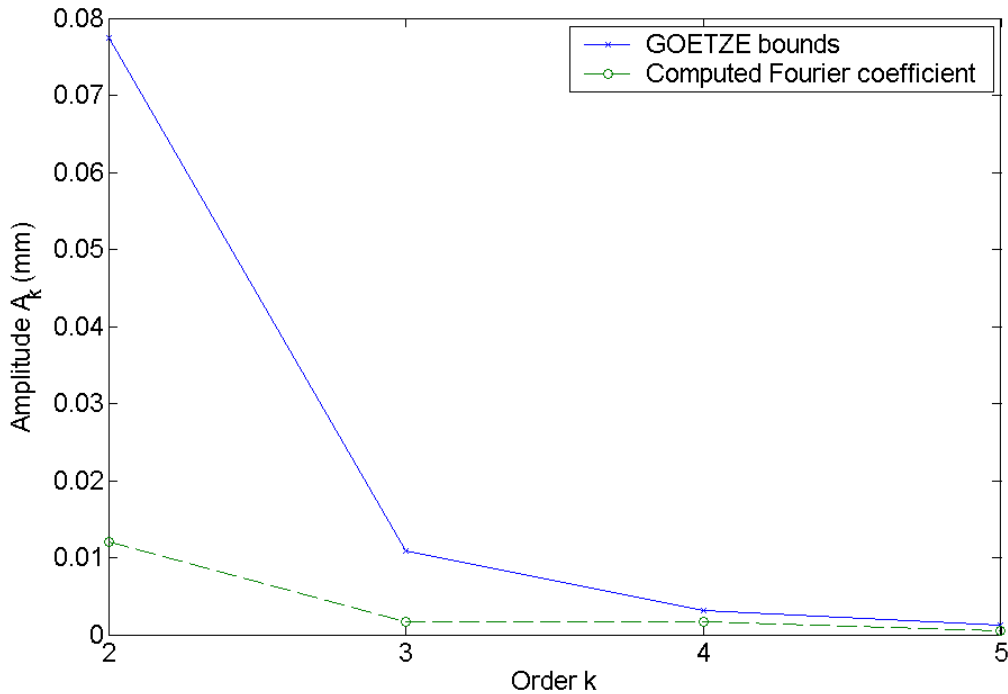


Figure 13. We compare the computed Fourier coefficients for FE data (deck 9) and the GOETZE bound (using the ring parameters in Table 2).

Discussion

Our numerical results let us assess the reliability of both the Dunaevsky and the GOETZE bounds. In Figure 9, we see that the bounds obtained via our simulation match the GOETZE bounds almost exactly. Although all three bounds match at second order, there is wide variation for higher orders. Since RINGPACK actually calculates each elastic variable with minimal approximation, this result suggests the GOETZE bounds are more accurate.

To explore this idea deeper, we derive the GOETZE bounds from first principles in Appendix B. Although Müller derived these bounds in [10], we provide a derivation since [10] is not available in English. Both the Dunaevsky [11] and GOETZE bounds use the same approximations of elasticity theory found in the Assumptions Section. However, Dunaevsky adds one additional assumption in his model.

Critical Curvature Assumption: The ring curvature at which the “light-tight” seal breaks is independent of order k .

That is, curvature induced by an oval distortion ($k = 2$) or a cloverleaf distortion ($k = 4$) will produce the same breach. However, the GOETZE derivation proves this assumption false. We see that pressure is dependent upon both curvature and the second derivative of curvature. Hence, small distortions of high order can produce large pressure

variations, while large distortions of low order may produce mild pressure variations. In fact, the GOETZE derivation gives an explicit formula for pressure in terms of radial distortions. For a k^{th} order distortion, the pressure is multiplied by a factor of $(k^2-1)^2$, thus magnifying pressure variations.

From our analysis, we must conclude that the Critical Curvature Assumption is unphysical. This false assumption leads the Dunaevsky bounds to overestimate conformability for orders three and beyond. Comparing the Dunaevsky to the semi-empirical Tomanik bounds, we see that the Dunaevsky bounds overestimate conformability to by more than 200%. However, the GOETZE bounds agree more closely with the semi-empirical results. Returning to Figure 9, we also see that the GOETZE bounds agree closely with our numerical study. From this evidence, the GOETZE bounds appear to predict conformability more accurately than the Dunaevsky bounds for high orders ($k > 3$). However, both the Dunaevsky and GOETZE bounds significantly overestimate conformability for second-order distortions, which we cannot explain.

After performing our parameter study, a natural question arises: what is the exact mathematical dependence of the second-order bound on ring thickness and radius? To answer this question, we assumed power law dependence and attempted to find the exponent. We used the standard approach: take the logarithm of dependent and independent variables and find the slope. We calculated slope by differentiating (via central differences) A_k with respect to both r_m and t . We then averaged the derivatives over the spatial grid. We determined that $A_2 \propto t^{-3}$ and $A_2 \propto r_m^3$. These sensitive dependencies agree with the results shown in Figure 10.

Comparing Figures 12 and 13, we note that a small breach has developed; however, the bore has not violated the GOETZE bounds at any order. In particular, it appears that the fifth-order contribution has contributed enough distortion to break the seal. From this example, we see the necessity of analyzing the entire bore profile. If we limit our analysis to an isolated Fourier harmonic, the bore “passes” the GOETZE bound; yet we see from Figure 12 that the negative pressure indicates a breach. Also, we note the unusually strong fifth-order contribution requires us to move beyond the standard four-term Fourier series approach [13].

We are also faced with an unanswered mathematical question: if we represent the bore profile via a Fourier series, how many terms should we use? Previous studies [4, 12] have terminated the Fourier series after the fourth term; this assumption was justified on physical grounds. However, as Figures 12 and 13 demonstrate, Fourier coefficients at fifth order and beyond may be present in a bore profile. We note that the current RINGPACK software shown in Appendix D is unstable for a large number of Fourier coefficients. In terms of conformability, the inclusion or exclusion of these high-order terms may lead to contradictory results. In fact, calculating the pressure for the example in Figures 12 and 13 with only four terms leads to a non-negative distribution. Hence, the problem of determining the “correct” number of Fourier coefficients is critical to understanding the present conformability problem.

Recommendations

Based on our research, numerical experimentation and data analysis, we recommend the following:

- Consider all orders of deformation simultaneously instead of only considering the dominant order.
- Investigate the relevance of deformation orders beyond four. Given particular engine and cylinder conditions, at what order should we terminate the Fourier series?
- According to our analysis, the GOETZE bounds predict conformability more accurately than the Dunaevsky bounds. Due to an unphysical assumption, the Dunaevsky bounds overestimate allowable distortion at high ($k > 2$) orders.
- Consider the effects of three-dimensional twist and combustion gas pressure in breaking/maintaining the “light-tight” seal.

Future Work

We hope to improve the accuracy of our conformability calculator by using more sophisticated derivative approximations. If time and funding permit, we will investigate the gas dynamic and lubrication problems encountered during engine operation.

Furthermore, we plan to obtain Finite Element code from the Engine Research Lab (ERL) as well as FEA programs used by DaimlerChrysler and compare the bounds we discussed to this data.

Acknowledgements

We would like to thank the following experts for providing helpful advice, data, insight and references:

- V. V. Dunaevsky, Bendix Corp
- Prof. Harold Schock, Engine Research Lab, Michigan State University
- Boon-Keat Chui, Engine Research Lab, Michigan State University

Bruce Geist at DaimlerChrysler was critical to the success of this project. He provided expertise in engine components and advanced mathematics, as well as encouragement and methods of attack.

We would like to express special gratitude to Prof. William Sledd for his support in various aspects of project implementation.

We also thank Prof. Clifford Weil, Department of Mathematics, Michigan State University for his assistance with our presentation at the Second Annual MSU Student Mathematics Conference.

References

- [1] Goetze AG, *Piston Ring Manual*, Burscheid, D-5093, 1989.
- [2] CASE Analysis System, "Theoretical Manual," Mid-Michigan Research, Okemos, MI, 2000.
- [3] F. P. Beer and E. R. Johnston, *Mechanics of Materials*, New York: McGraw-Hill Book Company, 1998, p. 221.
- [4] E. W. Scheider, "Effect of cylinder bore out-of-roundness on piston ring rotation and engine oil consumption," *Society of Automotive Engineers*, 930796, pp. 139-160, 1993.
- [5] S. H. Hill, "Piston ring designs for reduced friction," *Society of Automotive Engineers*, 841222, pp. 1-20, 1984.
- [6] J. Prescott, *Applied Elasticity*, New York, Dover Publications, 1946
- [7] S. Timoshenko, *Theory of Elastic Stability*, New York: McGraw-Hill, 1936.
- [8] C. Englisch, *KolbenRinge*, Vienna: Springer-Verlag, 1958.
- [9] Gintsburg, B. Ya, "Splitless-type piston rings," *Russian Engineering Journal*, Vol. 48, No. 7, pp. 37-40, 1968.
- [10] R. Müeller, "Zur grage des formuuellungsvermoegens von kolbenringen in von der kreisform abweichenden bohrungen gleicher umfanglaenge," *MTZ*, Vol 31, pp. 79-82, 1970.
- [11] V. V. Dunaevsky, "Analysis of distortions of cylinder and conformability of piston rings," *Tribology Transactions*, Vol. 33, No. 1, pp. 33-40, 1990.
- [12] K. Loenne and R. Ziemb, "The goetze cylinder distortion measurement system and the possibilities of reducing cylinder distortions," *Society of Automotive Engineers*, 880142, pp. 25-33, 1988.
- [13] S. Abe and M. Suzuki, "Analysis of cylinder bore distortion during engine operation," *Society of Automotive Engineers*, 950541, pp. 9-14, 1995.
- [14] M. A. Ejakov, H. J. Schock, and L. J. Brombolich, "Modeling of ring twist for an IC engine," *Society of Automotive Engineers*, 982693, 1998.
- [15] M .A. Ejakov, "Modeling of axial and circumferential ring pack lubrication," ASME, 2001, pp. 1-12.

- [16] V. V. Dunaevsky, J. T. Sawicki, J. Frater, and H. Chen, "Analysis of elastic distortions of a piston ring in a reciprocating air brake compressor due to the installation stresses," *Society of Automotive Engineers*, 013770, 2000.
- [17] V. V. Dunaevsky and S. Alexandrov, "Fundamentals for analysis of three-dimensional distortions of the piston rings," *Proceedings of the 2000 Fall Technical Conference of the ASME Internal Combustion Engine Division*, pp. 15-22
- [18] V. V. Dunaevsky, S. Alexandrov and F. Barlat, "Analysis of three-dimensional distortions of the pistons rings with arbitrary cross-section," *Society of Automotive Engineers*, 013453, 2000.
- [19] V. V. Dunaevsky, S. Alexandrov, "Development of conformability model of piston rings with consideration of their three-dimensional torsional distortions and Fourier series representation of cylinder bore geometry," *Society of Automotive Engineers*, 013453, 2002
- [20] V. V. Dunaevsky, S. Alexandrov and F. Barlat, "The effect of contact pressure on piston ring twist," *Society of Automotive Engineers*, 012720, 2001.
- [21] Love, A. E. H., *A Treatise on the Mathematical Theory of Elasticity*, 4th Ed., New York: Dover, 1927.
- [22] E. Tomanik, "Piston ring conformability in a distorted bore," *Society of Automotive Engineers*, 960356, pp. 169-180, 1996.
- [23] A. F. Ware, "Fast approximate Fourier transforms for irregularly spaced data," *SIAM Review*, Vol. 40, No. 4, pp. 838-856, December 1998
- [24] P. J. Davis and P. Rabinowitz, *Numerical Integration*, New York: Academic Press, 1975.
- [25] M. P. DoCarmo, *Differential Geometry of Curves and Surfaces*, Englewood Cliffs, NJ: Prentice-Hall, Inc., 1976.
- [26] Gintsburg, B. Y., *Theory of Piston Ring*, Mashinostroenie (Machinery Construction Publishing House), Moscow, 1979.
- [27] V. V. Dunaevsky and S. Alexandrov, "A 3-D Engineering Approach to Conformability Analysis of Piston Rings," *Society of Automotive Engineers* (accepted).

Appendix A: Free Shape Problem

During the derivation of the conformability criterion, Dunaevsky [11] makes the Free Shape Approximation. Here, $u(\phi)$ describes the free shape deviation from a perfect circle. In the following analysis, we relax this assumption in an attempt to quantify some of the error present in the Dunaevsky bounds by solving for the free-shape deviation u using an “exact” approach.

Instead of using the approximation found in [11], we use the exact formula (Equation 14) for the curvature of the uncompressed ring [25]:

$$\kappa_0 = \frac{(r+u)^2 + 2(u')^2 - (r+u)u''}{[(r+u)^2 + u'^2]^{3/2}}. \quad (\text{A1})$$

Now define the dimensionless quantity $\varepsilon = u/r$. Factor out an r and apply the definition to get

$$\kappa_0 = \frac{(1+\varepsilon)^2 + 2(\varepsilon')^2 - (1+\varepsilon)\varepsilon''}{[(1+\varepsilon)^2 + (\varepsilon')^2]^{3/2}}. \quad (\text{A2})$$

From Equation 12, we can calculate the free shape by using Equation 2. Pressure can be related to bending moment via the convolution integral

$$M(\phi) = hr^2 \int_{-\pi}^{\phi} p(\phi') \sin(\phi' - \phi) d\phi'. \quad (\text{A3})$$

For the special case of constant pressure p , we have the closed-form equation

$$M(\phi) = phr^2(1 + \cos\phi). \quad (\text{A4})$$

We can then solve Equation 2 for the dimensionless, free shape $\varepsilon(\phi)$ using Equations 12 and 14. The resulting equation is the following second-order, nonlinear ODE

$$\frac{(1+\varepsilon)^2 + 2\varepsilon'^2 - (1+\varepsilon)\varepsilon''}{[(1+\varepsilon)^2 + \varepsilon'^2]^{3/2}} = K(1 + \cos\phi) + 1, \quad (\text{A5})$$

subject to the initial conditions given below.

Initial Conditions: Displacements are the same at both ends of the ring. Then $u(0) = u(\pi) = Kr$ and $u'(0) = 0$.

Although an analytical solution for Equation A5 exists [2], it is expressed as a complicated infinite series involving Bessel functions. Evaluation of Bessel functions can be computationally expensive; therefore we chose numerical approach. Also analytical

solution exists for the uniform pressure distribution, while we might choose to extend our analysis to the non-uniform pressure distributions.

Table A1 shows the parameters used in our calculations.

In our calculations, we used $K = 0.0462$ and $r = 48.50$ mm. We solved Equation 15 numerically using a fourth-order, adaptive Runge-Kutta solver. We imposed the initial conditions and solved via the MATLAB solver `ode45`. See Appendix A for MATLAB code.

Figure A1 shows both the first-order approximation for u (given by Equation 4) and our exact solution. Note that the two functions deviate significantly, causing us to question the very foundations of the linear approach. Most importantly, there is a 15% relative difference at the end-gap of the piston ring. This is a significant deviation, and warrants further scrutiny.

We repeated the calculations with parameters from [11]. Figure A2 shows the results. Note that the relative difference at the end-gap exceeds 20% in this case.

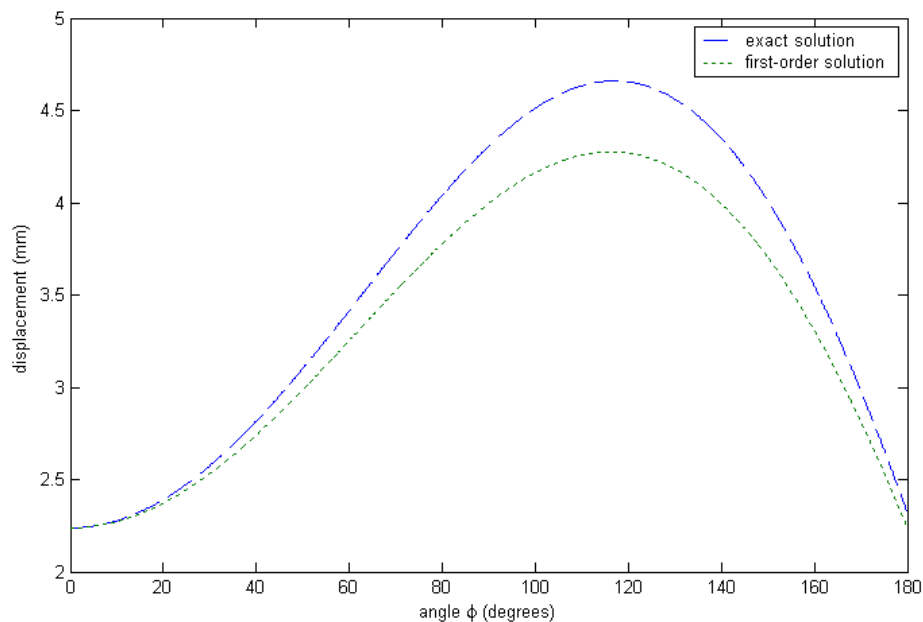


Figure A1. We display the first order approximation and the exact solution of the free-shape deviation of the piston ring using parameters from Tomanik [22].

Table A1. We display the physical parameters used in free-shape calculations.

Parameters	Dunaevsky	Tomanik
Diametrical Load (Q) (N)	15.76	110.4600
Height (mm)	1.597	2.4807
Thickness (mm)	1.625	3.64
Radius of curvature (mm)	18.44	48.5
Young's Modulus (N/mm ²)	11650	225000
Closing Force (N)	5.99	42.0
Moment of Inertia (mm ⁴)	.5711	9.97
Stiffness (mm ²)	66530	2240000
Conformability	.0306	0.0440

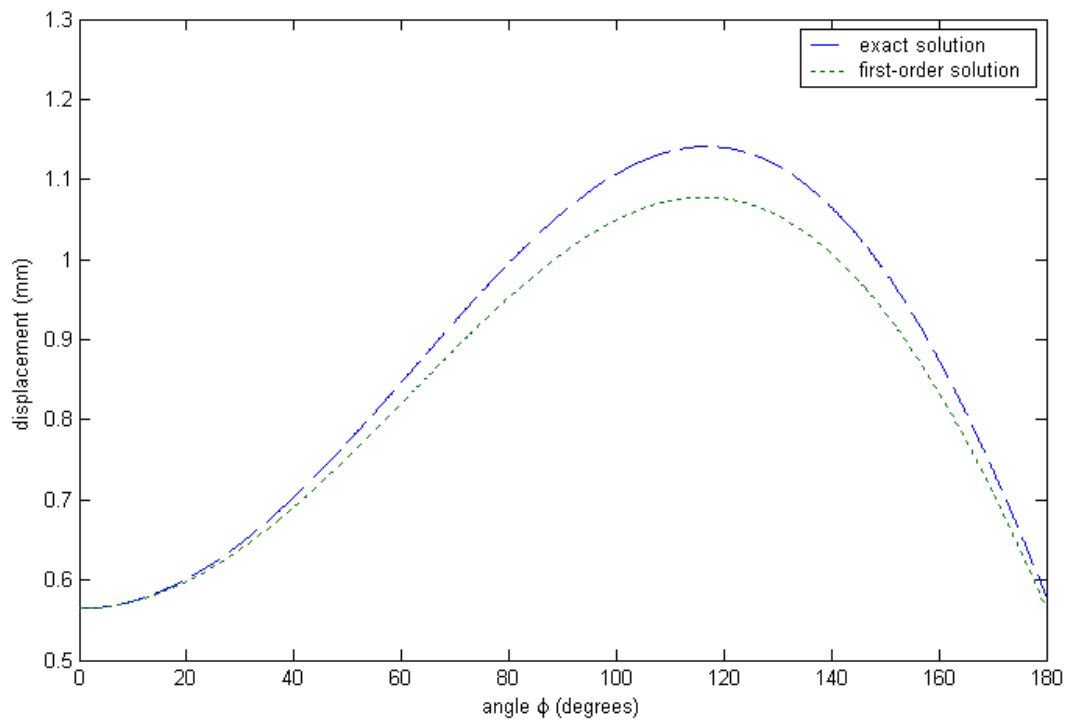


Figure A2. We display the first order approximation and exact solution of the free-shape deviation of the piston ring using parameters from Dunaevsky [11].

Appendix B: GOETZE Bound Deviation

We derive the GOETZE bounds based on first principles of elasticity theory. For extensive theoretical background, see [26]. Recall that the curvature of the ring in the free shape is given by (Equation 13):

$$\kappa_f = \frac{1 - K(1 + \cos\phi)}{r_0}, \quad (\text{B1})$$

where K is the conformability coefficient defined by Equation 3b and r_0 is the radius of the undistorted bore.

Equation 14 gives the curvature of the distorted bore in polar coordinates. Assuming that ξ'/ξ is negligibly small, we can simplify the formula to the form:

$$\kappa(\xi) \approx \frac{1}{\xi} - \frac{\xi''}{\xi^2}. \quad (\text{B2})$$

The bore profile ξ can be represented in polar coordinates as

$$\xi = r_0 + \varepsilon(\varphi), \quad (\text{B3})$$

where $\varepsilon(\varphi)$ is small deviation from the circular shape. Inserting Equation B3 into B2, decomposing into geometric series and using the fact that ε/r_0 is small ($\cong 0.05$) we obtain the formula for the curvature of the distorted bore (or compressed ring inserted into the distorted bore):

$$\kappa(\xi) \approx \frac{1}{r_0} - \frac{\varepsilon + \varepsilon''}{r_0^2}. \quad (\text{B4})$$

Since any physical bore profile can be expanded in Fourier series, assume the deviation $\varepsilon(\varphi)$ is the k -term of the Fourier series:

$$\varepsilon(\varphi) = A_k \cos(k(\varphi + \delta_k)), \quad (\text{B5})$$

where A_k is radial distortion amplitude, k is the order of distortion and δ_k is the phase.

We need to find the bending moment generated by compressing the ring from the free shape into the cylinder bore. Using the fundamental relation given by Equation 2 and substituting corresponding expressions for the curvatures given by Equations B2 and B4, we obtain (after inserting expression for $\varepsilon(\varphi)$ into Equation B4):

$$M(\varphi) = \frac{EI}{r_0^2} \left[Kr_0(1 + \cos\phi) + A_k(k^2 - 1)\cos(k(\varphi + \delta_k)) \right]. \quad (\text{B6})$$

Finally, we determine the pressure that the ring exerts on the bore using Equation 15. Substituting expression for the moment from Equation B6 into Equation 15 and simplifying, we attain the formula:

$$p(\varphi) = \frac{EI}{hr_0^4} \left[Kr_0 - A_k (k^2 - 1)^2 \cos(k(\varphi + \delta_k)) \right]. \quad (\text{B7})$$

We want to determine maximum A_k such that pressure is non-negative. The maximum value of cosine function is unity, so set the cosine term to unity and set pressure equal to zero. Solving for amplitude yields:

$$A_k = \frac{Kr_0}{(k^2 - 1)^2}. \quad (\text{B8})$$

Equation B8 corresponds with the GOETZE Bounds derived by Müller in 1970.

Appendix C: Three-Dimensional Distortion

So far we considered only two-dimensional distortions that occur in piston rings. But we can go further and build a conformability model in case of three-dimensional torsional distortions (or so-called *twist*) of piston rings. As a basis for this model we take the Dunaevsky's papers [16,17,18,19,20,27]. To build this model let us make some preliminary assumptions:

Assumption I: When ring is in the free state, the shape of centerline of ring differs from a perfect circle only insignificantly. Ratio of the radial thickness of the ring to its radius of the curvature is small. In free state, absent twist, all cross-sections of ring are identical.

Let τ_0 be the twist and k_0 be the curvature of the ring in the initial, uncompressed state. Then

$$\tau_0 = 0, \quad \kappa_0 = 1/r_0, \quad (C1)$$

where r_0 is the radius of the centerline in the initial state.

Assumption II: In the deformed state, the centerline of a ring is symmetrical about x-axis (see Figure C1). The maximum vertical displacement of any point of the centerline is small compared with a typical radius of the ring. A horizontal displacement of the centerline of the ring caused by twist is also small (compared with the vertical displacement) and can be neglected.

From this assumption, we can represent the centerline of the ring by Equation C1. For convenience we introduce the following dimensionless quantities: $R(\theta)/R_0$, where R_0 is the typical radius of the centerline and $v(\theta)/H$ where H is the maximum possible vertical displacement of any point of the cross-section. We retain notations $R(\theta)$ and $v(\theta)$ for these dimensionless quantities.

In his paper, Dunaevsky derives the formula for the infinitesimal element ds of the deformed centerline. Taking the initial general formula $ds = R_0 R \sqrt{1 + \left(\frac{R'}{R}\right)^2 + \left(\frac{\varepsilon v'}{R}\right)^2} d\theta$, assuming $(\varepsilon = H/R_0) \ll 1$ and neglecting $O(\varepsilon^2)$ term, the simplified formula will look like:

$$ds = R_0 R \sqrt{1 + \left(\frac{R'}{R}\right)^2} d\theta = R_0 a(\theta) d\theta,$$

where

$$a(\theta) = R \sqrt{1 + \left(\frac{R'}{R}\right)^2}. \quad (C2)$$

Also, Dunaevsky derived formula for the curvature k of the deformed ring:

$$k = \frac{\sqrt{g_1^2(\theta) + g_2^2(\theta)}}{R_0}. \quad (C3)$$

Here $g_1(\theta) = \frac{R''(\theta) - R'(\theta)}{a(\theta) \cdot a'(\theta)}$ and $g_2(\theta) = \frac{R''(\theta) + R'(\theta)}{a(\theta) \cdot a'(\theta)}$.

Further, Dunaevsky declares the system of equations describing given model:

$$\begin{cases} M_1 = A(k^{(1)} - k_0^{(1)}) \\ M_2 = B(k^{(2)} - k_0^{(2)}) \\ M_3 = C(\tau - \tau_0) \end{cases} \quad (C4)$$

where M_1 and M_2 are couples transforming the ring in plane perpendicular to bore axis, M_3 is torsional couple (one that causes twist), $k^{(1)}$ and $k^{(2)}$ are the components if k curvature vector in the principle torsion-flexure axes on each cross-section in the deformed state. That is if we take arbitrary cross-section of the ring (Figure C1) then for $k^{(1)}$ and $k^{(2)}$ we will have the following equations:

$$k^{(1)} = -k \cos \gamma, \quad k^{(2)} = k \sin \gamma, \quad (C5)$$

where γ is the twist angle for the particular cross-section. $k_0^{(1)}$ and $k_0^{(2)}$ are the components if k curvature vector in the initial state and τ is the twist in the deformed state.

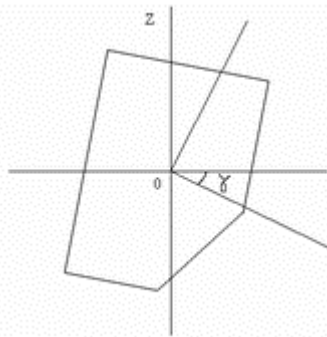


Figure C1. This figure shows an arbitrary cross-section of a piston ring. The angle γ denotes the twist angle.

The constants A , B and C in Equation C4 can be found for any cross-section of the ring. At this point, Dunaevsky attempts to solve the system C4 numerically.

Appendix D: RINGPACK Code

```
function [profile, angles]=importbore(layer,rm)
%loads grid and displacement data from "grid.dat" and
%"3L_stopper_displaced.dat"
% layer = deck to import
% rm = known radius of bore/ring
% profile = bore profile (radius as a function of angle)
% angles = angles for which profile is known

%load data files here (reverse ordering)
A=importdata('grid.dat');
A = flipud(A);
B=importdata('3L_stopper_displaced.dat ');
B = flipud(B);
len = length(A);

%get grid locations and each component of displacement
x0 = A(1:len,2); y0 = A(1:len,3); z0 = A(1:len,4);
dx0 = B(1:len,2); dy0 = B(1:len,3); dz0= B(1:len,4);

%Bottom and Top deck centers, given by Bruce
XCent = [-94.102, -94.102]; YCent = [66.2796, 166.268]; ZCent =
[66.0163, 166.072];
%the cylinder is titled in a V-engine, rotate s.t. parrallel with z-
axis
[THETA,RHO] = cart2pol(y0,z0);
[TH,PHI,R] = cart2sph(dx0,dy0,dz0);
tiltangle=atan((ZCent(2)-ZCent(1))/(YCent(2)-YCent(1)));
%tiltangle=pi/4;
THETA = THETA+tiltangle;
PHI = PHI + tiltangle;
x=x0;
[y,z] = pol2cart(THETA,RHO);
[dx,dy,dz]=sph2cart(TH,PHI,R);
[THETA,RHO] = cart2pol(YCent,ZCent);
THETA = THETA+tiltangle;
[YCent,ZCent] = pol2cart(THETA,RHO);

%extract the deck: deck 1 has 22 points, the other have 23
SP = 24*(layer-1); num = 23;
if layer == 1
    SP = SP+1; num = 22;
end

boreX = x(SP:SP+num); boreY = y(SP:SP+num); boreZ = z(SP:SP+num);
dispX = dx(SP:SP + num); dispY = dy(SP:SP + num); dispZ= dz(SP:SP +
num);
centX = XCent(1); centY = YCent(1); centZ = mean(boreZ);

%calculate radial component, through away the rest
for i=1:length(boreX)
    rv = [boreX(i)-centX, boreY(i)-centY];
    [angles1(i),grid(i)] = cart2pol(rv(1),rv(2));
```

```

    deltar(i)=cos(angles1(i))*dispX(i) + sin(angles1(i))*dispY(i);
end

%generate the profile (make sure angles are increasing)
prof = ([angles1;rm + deltar])';
prof = sortrows(prof);

angles = (prof(:,1))';
profile = (prof(:,2))';
function [a0,ak,bk]=fcoeffs_trighi(y,x,Ncoeffs)
%assume interval (-pi,pi)
%calculate Fourier coefficients from definition (NO FFT)
%use for irregularly spaced data
%use Gaussian quadrature

load gauss1to30;
NGauss=30;
yp=spline(x,y);

ak=zeros(1,Ncoeffs);
bk=zeros(1,Ncoeffs);
psi=pi.*abscissas(1:NGauss,NGauss);
w=pi.*weights(NGauss,1:NGauss);
term1=ppval(yp,psi);
a0=sum(w'.*term1)./pi;

for k=1:Ncoeffs
    term2=cos(k.*psi);
    term3=sin(k.*psi);
    ak(k)=sum(w'.*term1.*term2)./pi;
    bk(k)=sum(w'.*term1.*term3)./pi;
end

function y=fscurvature(A0,an,bn,theta)
%calculates exact curvature in polar coordinates of Fourier series
% an = cos terms
% bn = sin terms
% A0= DC component
% theta = interval of evaluation
[A0p,anp,bnp]=fsderv(A0,an,bn);
[A0pp,anpp,bnpp]=fsderv(A0p,anp,bnp);

x=fseval(A0,an,bn,theta);
xp=fseval(A0p,anp,bnp,theta);
xpp=fseval(A0pp,anpp,bnpp,theta);

num=x.^2 + 2.*xp.^2 - x.*xpp;
denom=(x.^2 + xp.^2).^(3/2);
y=num./denom;

function [A0p,anp,bnp]=fsderv(A0,an,bn);
%calculates derivative of Fourier series
A0p=0;
Ncoeffs=length(an);
k=1:Ncoeffs;
anp=k.*bn;

```

```

bnp=-k.*an;

function y=fseval(A0,an,bn,theta);
%evaluates a trigonometric Fourier series
% an = cos terms
% bn = sin terms
% A0= DC component
% theta = interval of evaluation
Ncoeffs=length(an);
y=(A0/2).*ones(size(theta));
for k=1:Ncoeffs
    y=y + bn(k).*sin(k.*theta) + an(k).*cos(k.*theta);
end

function pp = freeshapespline(rm,conform)
% returns the free shape as a natural cubic spline
% rm=middle radius
% conform=conformability
% calls ringsystem.m, which defines the ODE system
rm=48.5;
conform=.04;
y0=[conform ;0];
phi=[0 pi];
%we need to play with these
options=odeset('RelTol',1e-8);
[theta u]=ode45(@ringsystem,phi,y0,options,conform);
Nhalf=length(theta);
N=2*Nhalf -1;
theta2=zeros(N,1);

theta2(1:Nhalf)=-flipud(theta);
theta2(Nhalf + 1:N)=theta(2:Nhalf);
u2(1:Nhalf)=flipud(u(:,1));
u2(Nhalf + 1:N)=u(2:Nhalf,1);
u2=rm + rm.*u2;
pp=spline(theta2,u2);

function dydt = ringsystem(phi,y,conform)
%Calculates Cam shape of ring from exact theory
%used by freeshape.m and freeshapespline.m
source=1-conform.*(1+cos(phi));

dydt = [    y(2);
          ((1 + y(1))^2 + 2*y(2)^2 -source*((1+y(1))^2 +
y(2)^2)^1.5)/(1+y(1));
        ]

%ringparameters.m
%holds data for ring fitted on distorted bore

h=1.48      % h, ring height (mm)
t=3.985    % t (or a), piston ring thickness (mm)
rm=51.181  % r, piston ring OUTER radius (mm)

```

```

Q=13.2558    % Q, diametrical load (= Ft / 2.15)
E=1.52e+05   % E, modulus of elasticity (Mpa)
Ft=Q/2.15;   %use empirical formula
I=h.*t^3/12;
stiffness=E*I;           %stiffness
conform=Ft.*rm^2./stiffness;    %conformability
Area=h.*t;

%RINGPACK2 calculator
%calculates pressure distribution for a distorted bore
clear all;
ringparameters;           %loads parameters of ring
deck_number=7;
Ncoeffs=6;
[profile, angles]=importbore(deck_number,rm);
%profile=rm.*ones(size(angles));

Ntheta=256;
theta=linspace(-pi,pi,Ntheta);
delta_theta=2*pi/Ntheta;
[a0,ak,bk]=fcoeffs_trighi(profile,angles,Ncoeffs);
Ak=sqrt(ak.^2 + bk.^2);    %radial distortions
zeta=fseval(a0,ak,bk,theta);

kappa0=(1-conform.*(1 + cos(theta)))./rm;    %curvature of
free shape
kappal=fscurvature(a0,ak,bk,theta);    %curvature of
distorted cylinder

%now determine how the ring distortes
Moment=stiffness.*(kappal-kappa0);    %bending
moment
Momentp=zeros(size(Moment));
shear=Momentp./zeta;    %shear force
in the ring
Momentpp=zeros(size(Moment));
%finally, calculate the pressure distribution
Momentp=nd5p(Moment,delta_theta,Ntheta);
shear=Momentp./zeta;
Momentpp=nd5p(Momentp,delta_theta,Ntheta);

pressure=1./(h.*rm^2).*(Moment + Momentpp);
%fix this
rconvert=180./pi;
figure(1)
plot(rconvert.*theta,pressure,rconvert.*theta,zeros(size(theta)))
set(gca,'fontsize',17);
xlabel('polar angle \phi (degrees)');
ylabel('pressure (\muPa)');
title('pressure distribution of distorted ring');
axis([-180 180 -1 1])

```